

# Kent Academic Repository

## Full text document (pdf)

### Citation for published version

Worthing, M.A. and Laurence, Ray and Bosworth, L. (2018) Trajan's Forum (Hemicycle) and Via Biberatica (Trajan's Markets): An HHPXRF Study of the Provenance of Lava Paving in Ancient Rome (Italy). *Archaeometry*. ISSN 0003-813X.

### DOI

<https://doi.org/10.1111/arcm.12374>

### Link to record in KAR

<http://kar.kent.ac.uk/65583/>

### Document Version

Author's Accepted Manuscript

#### Copyright & reuse

Content in the Kent Academic Repository is made available for research purposes. Unless otherwise stated all content is protected by copyright and in the absence of an open licence (eg Creative Commons), permissions for further reuse of content should be sought from the publisher, author or other copyright holder.

#### Versions of research

The version in the Kent Academic Repository may differ from the final published version.

Users are advised to check <http://kar.kent.ac.uk> for the status of the paper. **Users should always cite the published version of record.**

#### Enquiries

For any further enquiries regarding the licence status of this document, please contact:

[researchsupport@kent.ac.uk](mailto:researchsupport@kent.ac.uk)

If you believe this document infringes copyright then please contact the KAR admin team with the take-down information provided at <http://kar.kent.ac.uk/contact.html>

# Trajan's Forum (Hemicycle) and Via Biberatica (Trajan's Markets): An HHPXRF Study of the Provenance of Lava Paving in Ancient Rome (Italy).

M.A. Worthing,<sup>1</sup> R. Laurence,<sup>2</sup> L. Bosworth<sup>1</sup>

## Abstract

The paper reports on geochemical data collected using a He-enabled Hand-Held portable XRF (HHPXRF) from lava paving stones in Trajan's Markets and Trajan's Forum (Rome). Issues relating to HHPXRF field use and calibration are also addressed in detail. Using this instrument 355 analyses of the paving stones were collected and the data was processed using the standard techniques of igneous petrology and petrography. Provenancing was based on comparisons between the HHPXRF data and geological data from the abundant literature on Roman volcanic rocks. These comparisons placed the provenance of the paving stones in the Alban Hills, southeast of Rome. Evidence is also presented pointing to possible source lava flows within the Alban Hills Complex. The study establishes the potential of HHPXRF equipment for non-destructive analysis of paving stones both in Rome and at other sites in central Italy and challenges a number of assumptions about the supply of building materials to Rome based on intuition alone.

## Introduction

Rome's hinterland, the middle and lower Tiber valley, is underlain by a variety of geological lithologies many of which were quarried in antiquity for construction projects. West of the river, lavas and pyroclastic rocks predominate whereas to east of the river, limestone, sandstones and conglomerate are the main rock types. These lithologies were generically known as '*silex*' in antiquity (Laurence 1999). However, the grey to black volcanic lavas, known as '*selce*' in the archaeological literature were the preferred rock type for paving in Rome and the roads of central Italy (Laurence 1999, 2004, Black et al 2004). Intuitively it might be expected that a heavy material such as lava would be quarried from local sources. However Capedri and Grandi (2003) presented lab-based XRF data suggesting that selce was transported up to 90 km to construction sites in the Po Plain from sources in the Euganean Hills. But, in general sourcing of paving stones in the archaeological literature has continued to be based on intuition rather than hard data (e.g. DeLaine 1997).

However, HHPXRF now provides a means of replacing these assumptions with hard data but few actual scientific studies have been undertaken. For example, Frahm and Doonan (2013) found that only 43% of archaeological papers using so called pXRF machines used handheld instruments (HHPXRF). These statistics are surprising particularly when considered against their use in other field based sciences such as the Earth Sciences (73%) and Environmental Testing (79%). More than four fifths of handheld pXRF analysis in archaeology is done in the laboratory and only 3% at an on-

---

<sup>1</sup> Department of Classical and Archaeological Studies, University of Kent, UK

<sup>2</sup> Department of Ancient History, Macquarie University, Australia

1  
2  
3 site laboratory and only 15% at an actual excavation. They attribute this partially to  
4 scepticism about the analytical performance of HHPXRF machines. In this paper, we  
5 have compared our HHPXRF analyses with lab-based XRF analyses of lava flows from  
6 the Alban Hills, Sabatini and Vico volcanoes taken from the geological literature. One  
7 of the advantages of this approach is that the geological data provides a reference  
8 standard against which the performance of the Niton HHPXRF can be assessed. This  
9 approach has also been enhanced by technological improvements, particularly in the  
10 development of He enabled machines, which permit the collection of a wider range of  
11 elements (compare Worthing et al 2017). The paper makes a contribution to developing  
12 a scientific basis for the provenancing of the lava paving from a major monumental  
13 complex in ancient Rome and the implications for the supply of building materials.  
14  
15

## 16 **Geological Background**

17  
18 The present day geological and physiographic framework of the Italian peninsula is a  
19 consequence of movements associated with the evolving Apennine Orogenic Belt  
20 (Conticelli et al. 2010a, Alagna et al. 2010). These movements began in the Eocene  
21 with convergence and westward subduction of Adriatic lithosphere beneath the  
22 southern European margin. This was followed by Miocene subduction related  
23 magmatism along the Italian peninsula which has continued to the present day. These  
24 magmatic rocks have been assigned to three magmatic provinces; from north to south,  
25 the Tuscan Magmatic Province (TMP), the Roman Magmatic Province (RMP) and the  
26 Lucanian Magmatic Province (LMP). In this paper we will only consider the RMP  
27 which comprises four volcanic complexes: Vulcini, Vico, Sabatini and the Alban Hills.  
28 These volcanoes lie along the border of the Tyrrhenian Sea between southern Tuscany  
29 and the south eastern hinterland of the city of Rome. In this paper three volcanoes of  
30 the RMP will be discussed: from north to south they are Vico, Sabatini and the Alban  
31 Hills but the main focus will be on the latter (Fig. 1).  
32  
33  
34

35 Vico, Sabatini and the Alban Hills are all characterised by large polycentric stratiform  
36 complexes with polygenetic calderas (Fig.1). Their eruptive products are dominated by  
37 voluminous explosive pyroclastic rocks such as ignimbrites and tuffs. Lava flows are  
38 subordinate. Geochemically these products are characterised by high levels of LILE  
39 (Large Ion Lithophile Elements) such as K, Rb, Sr, Ba and Pb relative to HFSE (High  
40 Field Strength Elements) such as Nb, Zr and Ti (e.g. Conticelli et al. 2010a, Alagna et  
41 al. 2010, Gaeta et al. 2016). The relative abundance of potassium and the  
42 undersaturation with respect to SiO<sub>2</sub> gave rise to the common occurrence of the potassic  
43 feldspathoid leucite. Texturally the lavas range from aphyric to strongly porphyritic with  
44 leucite, clinopyroxene, plagioclase and olivine as common phenocryst phases.  
45 Geochemical classification of these rocks has divided them into two suites; a potassic  
46 suite consisting of trachybasalts and trachytes and an ultrapotassic suite consisting of  
47 foidites, leucitites, leucite tephrites and phonolites (Alagna et al. 2010).  
48  
49  
50

## 51 **The Alban Hills**

52  
53 This volcanic complex lies 15km southeast from the centre of Rome and much of the  
54 city is built on its eruptive products (Fig.1). Activity was dominated in the early phases  
55 by polygenetic caldera collapse and the eruption of voluminous explosive products such  
56 as ignimbrites and tuffs some of which are interbedded with coeval tuffs from Sabatini  
57 (Conticelli et al. 2010a, Gaeta et al 2016). Lava flows are subordinate and the volume  
58  
59  
60

1  
2  
3 of eruptive products decreased with time. In this paper we have adopted the  
4 terminology of Gaeta et al. (2016) to describe the magmatic phases of the volcano.  
5 They are an Early Tuscalano-Artemisio Phase (608 – 500 ka), a Late Tuscalano-  
6 Artemisio Phase (456 - 351 ka), the Monte Delle Faete Phase (308 – 241 ka), a Late  
7 Hydromagmatic Phase (201 – 142 ka) and finally the Albano Phase (69 – 40 ka).  
8

9  
10 Of particular interest to this paper are lava flows of the Monte Delle Faete Phase (Fig.  
11 1). The Late Tuscalano-Artemisio Phase (Fig. 1) also hosts significant lava flows  
12 including the Villa Senni lavas and the lavas of the Pozzolane Rosse which were  
13 erupted on the Vallerano lava plateau (Fig.1). Similarly, the Monte due Torri flow of  
14 the Albano Phase is the most recent lava erupted from the Alban Hills and was dated at  
15 40 ka (Gaeta et al. 2011). These lavas are all possible sources for some of the paving  
16 stones documented in this paper.  
17

### 18 **Sabatini**

19  
20 The picture here is more complex mainly because overlapping eruptions occurred from  
21 multiple sources including three major caldera complexes; Bracciano, Baccano and  
22 Sacrafano together with scoria cones and hydromagmatic maar activity (Conticelli et al.  
23 1997, 2010a, Karner et al.2001, Sottili et al. 2010, Marra et al. 2014) (Fig.1). Activity  
24 was dominantly explosive occurring between 800 and 86ka producing voluminous  
25 pyroclastic flows and tuffs. In the south east some of these are interbedded with tuffs  
26 from the Alban Hills (Marra et al 2011). Lava flows occur at a number of scattered  
27 localities (Fig. 1). The most intense monogenetic activity was concentrated at  
28 Trevignano areas to the north of the Bracciano crater, at Monte Maggiore close to the  
29 Sacrofano caldera, and at Monte Aguzzo and in the southeast. and at San Selso south of  
30 Bracciano crater. (Fig.1).  
31  
32

### 33 **Vico**

34  
35 This consists of a single conic stratiform volcano with a central caldera containing the  
36 crater lake of Lake Vico (Fig.1). The magmatic products of Vico have been divided  
37 into three main rock Successions (Perini et al. 2000, 2004, Conticelli et al. 2010a). The  
38 Rio Ferriera Succession began at about 420 ka with the production of pyroclastic fall  
39 deposits with interbedded lava flows. The Lago di Vico was a stratovolcano building  
40 phase with some interbedded lava flows (300 ka – 260 ka) followed by four explosive  
41 ignimbrite eruptions which destroyed the earlier Vico edifice and formed the current  
42 caldera. The Monte Venere Succession was a post-caldera phase ranging in age from 95  
43 to 85 ka. and was characterised by tuffs and minor lava flows.  
44  
45  
46

## 47 **Methodology**

### 48 **Calibration of HHpXRF Equipment**

49  
50 Geochemical data for this paper was collected using a hand held Niton XL3t 950 He  
51 GOLDD+ X-ray analyser (hereafter referred to as “the Niton”). We learned from our  
52 first project using the earlier Niton XLt 792 MZ machine that good calibration is vital  
53 to the successful use of the analyser (Worthing et al. 2017). The XL3t 950 machine  
54 comes with factory calibrations that may have to be customised for specific tasks. This  
55 was particularly important in this project as determination of paving stone provenance  
56  
57  
58  
59  
60

1  
2  
3 depended on comparisons between Niton data and data sourced from the geological  
4 literature of the Roman Volcanic Province. This was obtained on lab-based XRF  
5 machines and ICPMS which are both capable of producing highly accurate analyses but  
6 require the collection and destruction of some of the rock sample. The paving stones  
7 investigated in this paper have a complex geochemistry consisting of about twenty  
8 seven different detectable elements that are part of a complex silicate matrix.  
9 Concentrations range from 20 element % down to 20 ppm. Thus careful calibration was  
10 required.  
11

12  
13 Our calibration protocol involved a number of steps. Firstly we investigated the  
14 accuracy of the factory calibrations. This required a rock standard of known  
15 composition against which Niton analyses could be compared. For this purpose we  
16 selected a discarded aphyric lava cobble stone (COB1) from a modern road in central  
17 Rome. This was analysed on a lab-based XRF machine at the University of Greenwich.  
18 Major elements were determined on a fused disc and trace elements on a pressed pellet.  
19 Significant geochemical features of this rock included a high  $K_2O/Na_2O$  ratio  
20 suggesting that it was sourced from a local volcano of the RMP and was therefore  
21 likely to be compositionally similar to the paving stones that are the subject of this  
22 paper.  
23

24  
25 We then measured ten analyses of COB1 on a flat sawn surface using the shielded test  
26 stand with the Niton set to factory calibrations. Data was collected in element % and  
27 major elements except P and Ti were converted to the geological format of Wt% oxide.  
28 Trace elements, Ti and P were converted to ppm. The ten analyses were averaged and  
29 are plotted in Figures 2a-c against the equivalent lab-based XRF analyses of COB1. A  
30 perfect calibration would show all elements plotting on the 1:1 line but deviations from  
31 this line would indicate faulty calibration. For example, Figure 2a shows that  $MgO$ ,  
32  $K_2O$ ,  $CaO$  and  $FeO$  are well calibrated although  $Al_2O_3$  deviates slightly from the 1:1  
33 calibration line. However,  $SiO_2$  is very poorly calibrated. Figure 2b shows that Sr and  
34 Ti are also poorly calibrated whereas P, Ba, Ce and Nd are reasonably constrained. In  
35 Figure 2c Rb and Zr are poorly calibrated but Cu, Zn, Pb, Y, and Nb are satisfactory.  
36 These graphs thus provide a visual check on the accuracy of the factory calibration.  
37  
38

39  
40 The third recalibration step required a number of standards of known composition.  
41 These were kindly provided by Dr Christine Manning who donated seven small chips  
42 of porphyritic Icelandic basalts that had been fully analysed by a lab-based XRF. These  
43 chips had one flat sawn surface which could be analysed by the Niton in the shielded  
44 test stand. Ten analyses of each chip were obtained and an average calculated. The  
45 Niton data for each sample was compared graphically with the equivalent data obtained  
46 by the lab-based XRF. The resulting 7 point graph for K and Fe are shown in Figure 3 a  
47 and b. They include the straight-line equations for the calibration curve and the  $R^2$   
48 value. The slope and intercept values from all equations were then fed into the  
49 CALFAC programme in the Niton software producing an element calibration file which  
50 we called BIBROCEL. This was loaded into the Niton memory and 10 analyses of  
51 COB1 were collected. An average was calculated from this data and the results are  
52 presented in Figures 2d-f alongside the factory calibration files. Figure 2d shows that  
53 the major elements are well calibrated. In particular  $SiO_2$  is much improved from the  
54 uncalibrated value shown in Figure 2a. There is also some improvement in the trace  
55 elements Ba and Sr, particularly the latter (Fig. 2e). Ti is slightly moved on the diagram  
56 but not much changed. P is actually worse. Figure 2f shows the other trace elements  
57  
58  
59  
60

1  
2  
3 Cu, Zn, Y, Pb and Nb which are well calibrated. Rb and Zr are improved but still not  
4 well constrained.  
5

6 The whole calibration protocol was repeated with seven basalt and andesite standards  
7 used in the XRF machine at the University of Greenwich. These standards were  
8 prepared from crushed rock powder mounted in a resin and therefore have a different  
9 matrix to the natural rock chips described above. Using this data we produced a second  
10 CALFAC file called BIBSTANEL which was saved as a separate file in the CALFAC  
11 programme and was used to re-analyse COB1. We found that BIBROCEL yielded the  
12 best results and accordingly we used this calibration file in the field.  
13  
14

15 During field work a sawn piece of COB1 was used as an external standard to monitor  
16 any drift in the Niton's performance. This exercise suggested that under field conditions  
17 of ambient temperatures of around 30°C and relatively high humidity, the Niton drifted  
18 from the original BIBROCEL calibration. For example, values for Ti, Fe, Mg and Ca  
19 were all high when compared with the lab-based XRF values for COB1. Thus on return  
20 to the University of Kent we repeated the calibration procedure outlined above in  
21 modified form. We selected three of the Icelandic basalts representing a range of SiO<sub>2</sub>  
22 values and together with COB1 re-analysed the samples using BIBROCEL. Four  
23 analyses of each sample were measured and averages calculated. These values were  
24 plotted on the CALFAC calibration graphs against the equivalent lab-based XRF values  
25 producing equations for each element. These equations were then used to correct the  
26 Rome field data in an EXCEL file. The resulting data was loaded into MinPet 2.02 for  
27 analysis.  
28  
29

### 30 **Sampling and Data Collection**

31  
32 Photographs taken at the time of excavation identified the Hemicycle of Trajan's  
33 Forum and the Via Biberatica as sections of ancient paving that had not been restored  
34 post-excavation. The tight fit of the paving stones can be seen to be indicative of paving  
35 from antiquity, whereas restoration work was characterised by gaps or cement fill  
36 (Fig.4a). Three areas of paving stones of the Hemicycle in Trajan's Market were  
37 selected for geochemical analysis in 2016 together with re-analysis of some paving  
38 stones in Via Biberatica. The stones were selected to ensure that the petrographic types  
39 identified on the previous visit were represented. It was apparent that the stones in the  
40 Hemicycle were more pitted, weathered and dirty than those on the Via Biberatica.  
41 Representative photographs are presented in Figure 4a-f. In addition, vertical  
42 photographs were taken of the three Hemicycle areas from overlooking balconies and  
43 these were used as accurate maps enabling location and numbering of each paving  
44 stone. We used the same numbering system for the Via Biberatica utilised in 2014.  
45  
46  
47

48 A small area of each paving stone was thoroughly cleaned by scrubbing with a plastic  
49 brush and clean water. Residues were wiped away with cosmetic wipes. This was  
50 followed by further cleaning with 99% ethanol to remove any organic residues and to  
51 dry the area prior to analysis. A small adhesive label with the paving stone number was  
52 then attached to the stone with an arrow pointing at the cleaned area (Fig. 4c).  
53 Discolouration of the discarded wipes indicated that the stones were generally very  
54 dirty. This was particularly the case for stones in the Hemicycle where pitting  
55 sometimes made it difficult to find a suitable flat surface for analysis. In order to  
56 investigate the effects of cleaning, ten samples were selected at random for analysis of  
57  
58  
59  
60

1  
2  
3 both the cleaned and uncleaned areas. This data shows that in many cases the analytical  
4 values obtained on the uncleaned areas were greater than those on the cleaned area.  
5 This was attributed to an accumulation of dust and pollution on the uncleaned surfaces  
6 and emphasised the importance of cleaning prior to analysis  
7

8  
9 As noted above, geochemical data was collected using a hand held Niton XL3t 950 He  
10 GOLDD+ X-ray analyser. The machine has an Au anode (9-50kV, 0-40 :A max) giving  
11 a resolution of <185eV. The He attachment permits determination of lighter elements  
12 such as Si, Al, Ca, Mg, P and K as well as elements between Ti and Bi on the periodic  
13 table: Zr, Sr, Rb, Ba, Pb, Fe, Mn, As, Zn, Cu, Ni, Nb, S, Pb, Th, La, Ce, Pr and Nd. The  
14 data set included 236 analyses from the three areas of the Hemicycle (Areas 1, 2 and 3)  
15 plus 119 analyses from the Via Biberatica. During analysis only matrix compositions  
16 were measured, phenocrysts were ignored and data was collected in element % using a  
17 livetime of 120 seconds. The lighter elements accessible with the XLt 950 allow  
18 presentation of data in a similar format to that used in the geological literature. This  
19 facilitated the comparisons required for sourcing. We also took 10 readings from a  
20 number of phenocrysts that characterise most of the lava paving stones.  
21  
22

### 23 **Paving Stone Petrography**

24  
25 Petrographic analysis was conducted on paving stones from the three areas in the  
26 Hemicycle. This data complemented a similar analysis undertaken on the Via  
27 Biberatica in 2014. A simple system was devised (modified after Browning  
28 unpublished) based on the presence or absence of phenocrysts, their modal percentages,  
29 grain size and the presence or absence of flow foliation. Table 1 describes the  
30 petrographic features used to classify the Groups present in the sample. The distribution  
31 of the different petrographic types among the three areas of the Hemicycle and the Via  
32 Biberatica are shown in Figures 5a-d. These histograms show that the three areas of the  
33 Hemicycle (Figs 5a-c) are very similar. The dominant rock types are grey porphyritic  
34 lavas with phenocrysts ranging between 1 to 5% by volume. (Figs 4b and c). Also all  
35 three areas have some stones showing flow foliation (Fig. 4d). The distribution of rock  
36 types in the Via Biberatica is more complex although again, the grey porphyritic types  
37 predominate. This complexity may possibly reflect the use of multiple source quarries  
38 or reuse of stones from other sites. An unusual group, present only on the Via  
39 Biberatica is coarser grained, with orange-weathering and was classified as Group 4A  
40 (Fig. 4e). The coarse grain size suggests that the rock may have been quarried from  
41 intrusions such as dykes. A distinctive feature of this rock type is the presence of  
42 curved, branching, randomly oriented acicular crystals probably of clinopyroxene. A  
43 few Group 4A stones showed evidence of the coarser grained rock type in an apparent  
44 intrusive relationship with the finer grained grey leucitic lava type (Fig. 4e). However  
45 the geochemistry of the two types appears to be identical suggesting that they were  
46 derived from the same magma.  
47  
48  
49  
50

51 The areal distribution of the different petrographic types is shown in Figs. 6 a-d. These  
52 diagrams were prepared from the vertical photographs and reveal some information  
53 about the distribution of the different rock types, particularly in the Hemicycle, from  
54 which tentative conclusions are drawn. Area 1 contains more of the 3A3 group than  
55 Areas 2 and 3. The latter are dominated by the 3A1 and 2 types. There is some evidence  
56 of clustering, particularly in Area 1 where 3A3 types are much more common. This  
57 may reflect the unloading of a group of similar stones collected perhaps from the same  
58  
59  
60

1  
2  
3 part of a lava flow in the source quarry. Foliated types such as 3AC2 are present in all  
4 three areas but are most abundant in Area 3 where they again tend to show clustering.  
5 Again this may suggest collection and unloading of lava blocks from a particular part of  
6 a lava flow.  
7

8  
9 The diagrams in Figure 6 are all drawn at the same scale and suggest that there are  
10 variations in the size of the stones. This was confirmed by numerical computer analysis.  
11 Area 1 shows the largest stones and the 3AC2 type is common. These differences may  
12 reflect choices made by the stone masons in response to the workability of the different  
13 types of lava. The foliated types in Area 1 may have been more susceptible to splitting.  
14 Four stones in Area 3 of the Hemicycle contain xenoliths (e.g. Fig.6a), a feature not  
15 present in Areas 2 and 3 and the Via Biberatica. They are described in some detail in  
16 the study by Tregila et al. (1995) on the geology of the Alban Hills and appear to be  
17 particularly common in the Villa Senni eruptive unit.  
18

19  
20 The geological literature suggests that one of the characteristic features of lavas from  
21 the Alban Hills is the ubiquitous presence of leucite phenocrysts (e.g. Tregila et al.  
22 1995). Thus we considered that it was important to confirm the identity of the  
23 ubiquitous phenocrysts in the Hemicycle and the Via Biberatica. The crystals are white  
24 or cream in colour and are often equant or square-shaped and up to 2cms in diameter.  
25

## 26 **Results and Analysis**

27  
28  
29 The aim of the research was to determine the composition of the paving stones and to  
30 use this information to establish their possible source or sources. Thus as a first step the  
31 composition of rocks from the three volcanoes close to Rome was investigated using  
32 the abundant geological literature on the Roman Magmatic Province (RMP). Thus 188  
33 analyses from the Alban Hills, Sabatini and Vico were loaded into MinPet software.  
34 (Trigila et al. 1995, Conticelli et al. 1997, Perini et al. 2000, 2004), Peccerillo 2005,  
35 Giordano et al. 2006, Conticelli et al. 2007, Boari et al. 2009, Marra et al. 2009, Alagna  
36 et al. 2010, Conticelli et al. 2010 a and b, 2010b, Gozzi et al. 2012, Gozzi et al. 2014,  
37 Gaeta et al. 2016).  
38

39  
40 All of these volcanoes have complex histories and in the case of Sabatini there are  
41 several eruptive phases and two major geochemical suites, a high Ba and a low Ba suite  
42 (Conticelli et al. 1997). The latter do not contain leucite so they were eliminated from  
43 the data set leaving 25 analyses. These are supplemented by 73 analyses from Vico and  
44 90 from the Alban Hills. The analyses were processed with Minpet petrological  
45 software using standard X-Y variation diagrams. The leucitic lavas are identified on the  
46 diagrams by colour coded triangles specific to the volcano from which they were  
47 erupted; green for the Alban Hills, blue for Sabatini and black for Vico. This data is  
48 shown in Figures 7a-f where the major elements  $\text{TiO}_2$ ,  $\text{Al}_2\text{O}_3$ ,  $\text{FeO}_T$ ,  $\text{MgO}$ ,  $\text{CaO}$ ,  $\text{K}_2\text{O}$   
49 and  $\text{P}_2\text{O}_5$  plotted against  $\text{SiO}_2$  and Figure 8a-g in which the trace elements Zr, Sr, Ba,  
50 Rb, Cu, and Pb are also plotted against  $\text{SiO}_2$ . The diagrams show the geological data  
51 spread across the diagrams with the Alban Hills data at the low  $\text{SiO}_2$  end, Vico at the  
52 high  $\text{SiO}_2$  end and Sabatini in the middle. There is some overlap between the Alban  
53 Hills and Sabatini data. In most cases the Alban Hills major and minor elements show  
54 elevated values relative to those of Sabatini and Vico. In each diagram the Alban Hills  
55 concentrations are enclosed by a field which includes most of the data points.  
56  
57  
58  
59  
60



1  
2  
3 The Niton data was converted to Wt% oxide for the major elements and ppm for trace  
4 elements. Figures 9a-g and 10a-f show the Via Biberatica and Hemicycle data plotted  
5 in the same X-Y plots as the geological data above. The Via Biberatica (VB) data is  
6 represented by green circles and the Trajan's Market Hemicycle (TM) data as red  
7 circles. The VB data tends to cluster whereas the TM data is slightly more spread. The  
8 linear trends shown in these diagrams are probably related to magmatic differentiation  
9 (e.g. Boari et al. 2009, Gozzi et al. 2014). In addition, the fields defining the Alban  
10 Hills clusters in Figures 7 and 8 above are also included. It is clear that these fields  
11 contain some or most of the VB and TM data. This is compelling evidence that the  
12 paving stones were sourced in the Alban Hills. There is, however, a note of caution.  
13 Close examination of Figures 7 and 8 show that nine Sabatini samples lie within the  
14 Alban Hills fields suggesting that they are geochemically identical to some of the rocks  
15 from the Alban Hills (see below for discussion).  
16  
17

### 18 **Phenocryst Compositions**

19  
20 As noted above leucite is a common phenocryst phase in many lavas from the RMP  
21 particularly the Alban Hills (e.g. Tregila et al. 1995) We used the Niton in toggle spot  
22 mode to obtain ten in situ analyses of some of the larger crystals, five from the Via  
23 Biberatica and five from the Hemicycle. The analyses were averaged and are presented  
24 in Table 2 together with two microprobe analyses from the Alban Hills (Boari et al.  
25 2009). The VB and TM Niton analyses in Table 2 were obviously measured under less  
26 than ideal conditions i.e on uneven pitted surfaces and not *in vacuo*. However the  
27 similarities are clear although some of the values such as Al<sub>2</sub>O<sub>3</sub> and SiO<sub>2</sub> are low.  
28 However given the analytical conditions we conclude that the phenocrysts are leucites.  
29  
30  
31

### 32 **Spider Diagrams**

33  
34 In the above section we have shown that standard X-Y petrological diagrams reveal a  
35 close relationship between the geochemistry of the Hemicycle and Via Biberatica  
36 paving stones and geological data for the Alban Hills. However the restriction of these  
37 diagrams to comparisons between two elements or element ratios limits their  
38 discriminatory power, in this case to a particular volcano. In igneous petrology, multi-  
39 element diagrams called spider diagrams are frequently used to discriminate between  
40 rocks from different tectonic settings. These diagrams employ large numbers of  
41 elements thus greatly improving their analytical power. They are based on comparisons  
42 between a geochemical data set and a calculated standard. For example in this paper we  
43 wished to compare the Niton data sets from Trajan's Market Hemicycle and the Via  
44 Biberatica with the different rock units from the Alban Hills, a process called  
45 normalisation. Thus, normalising standards were calculated for each of the effusive  
46 phases from the Alban Hills as defined by Gaeta et al. (2016). These standards were  
47 calculated as follows: the average of nine samples from the Pozzolane Rosso lavas from  
48 the Vallerano Plateau (AvVal) (Gaeta et al. 2006, Boari et al. 2009, Marra et al. 2009,  
49 Gozzi et al. 2014), three samples from the Villa Senni lavas (AvSen) (Marra et al. 2009,  
50 Gozzi et al. 2014, Gaeta et al. 2016), twenty two samples from the Monte della Faete  
51 lavas (AvFaet) (Boari et al. 2009, Marra et al. 2009, Gozzi et al. 2014, Gaeta et al.  
52 2016) and one sample from the Monte due Torri lavas (AvTorri) (Gaeta et al. 2011).  
53 The elements to be compared with the standards were placed at the bottom of the  
54 diagram. They are Si, Ti, Al, Fe, Mg, Ca, K, P, Rb, Sr, Zr, Ba, Pb, Y and Nb. The  
55 MinPet software divided the concentrations of these elements in the paving stones with  
56  
57  
58  
59  
60

1  
2  
3 the appropriate standard value (i.e. the ratio Sample/Standard was calculated). This  
4 value was plotted above each element on a vertical logarithmic scale. Thus elements  
5 with the same concentrations as the standard will plot as a value 1. Thus the similarity  
6 to the standard of the selected elements can be visually assessed.  
7

8  
9 Figure 11a-d shows a series of spiders plotted in which the Via Biberatica (green) and  
10 the Hemicycle data (red) are compared with the different Alban Hills standards. They  
11 all plot close to the line 1 showing that their geochemistry are very similar to the Alban  
12 Hills standards. However the flattest curve is the one for the Vallerano lavas (Fig. 11a)  
13 The Pb values are anomalous showing positive spikes (Figs. 11 a-c). However we have  
14 suggested before (Worthing et al. 2017) that paving stones from urban areas appear to  
15 be contaminated with atmospheric lead giving rise to anomalous Pb spikes. In the case  
16 of Figure 11d, the Monte due Torri lava has an unusually low Pb concentration (6ppm)  
17 which together with atmospheric contamination, has given rise to the large positive  
18 spike. We can therefore conclude that both the X-Y plots (Figs. 9 and 10) and the  
19 spiders of Figures 11a-d suggest that the Via Biberatica and the Hemicycle paving  
20 stones were sourced in the Alban Hills. However, it is clear that the similarity of the  
21 diagrams means that they fail to discriminate between the different effusive units that  
22 were used to normalise the data. We will attempt to address this issue below.  
23  
24

### 25 **Zr/Y vs Nb/Y discriminant diagrams**

26  
27 Rock materials such as lavas, tuffs and pozzolane were used extensively in the  
28 architecture of Roman masonry and concretes (e.g. DeLaine 1997, 2000; Marra et al.  
29 2011). These authors showed that in many cases the primary geochemistry of these  
30 rocks, particularly of tuffs and pozzolane has been modified by element mobility during  
31 Quaternary weathering and pedogenesis. Clearly, these changes in geochemistry  
32 complicate the sourcing of these materials. In response, Marra et al. (2011) devised a  
33 set of discriminant diagrams based on the trace elements ratios Zr/Y vs Nb/Y and  
34 Th/Ta vs Nb/Zr. These elements tend to be immobile during weathering and can thus be  
35 used to document both the primary geochemistry of the deposits and the vectors of  
36 geochemical change in measured sections in the Alban Hills and Monte Sabatini. They  
37 were also used to facilitate sourcing of construction materials  
38  
39

40  
41 Figure 12a shows a plot of Zr/Y vs Nb/Y for samples identified as belonging to the  
42 principle effusive phases of the Alban Hills used in the spider diagrams of Figure 9  
43 (Gaeta et al. 2016). They are as follows: the Monte della Faete lavas, the Monte due  
44 Torri lavas, the Vallerano lavas and the Villa Senni lavas (Fig. 1). The data was  
45 abstracted from geological analyses and clusters into four overlapping fields. Figure 12  
46 b. shows a plot of the Niton data from the Via Biberatica and the Hemicycle using the  
47 same ratios together with the fields from Figure 12a. The vertical linear distribution of  
48 the data in Figure 12b is probably a function of the fact that the data for these two  
49 elements is close to the detection limits of the Niton. It thus tends to cluster tightly  
50 around the small range of 30-40ppm for Y and 20ppm for Nb. However when the data  
51 for these two elements is normalised to the geological data in the spiders of Figures 11,  
52 they plot close to 1 indicating that their concentrations are close to the values in the  
53 geological data set. We consider that this validates their use as described above.  
54  
55

56  
57 Inspection of Figures 12a and b shows that they do not clearly discriminate between the  
58 different possible sources on the Alban Hills. However a number of comments are  
59  
60

1  
2  
3 possible. Firstly the two main data clusters in Fig. 12b suggest that lavas from at least  
4 two sources were used in the Via Biberatica and the Hemicycle but their distribution in  
5 these sites is numerically different. For example, the higher ratio cluster contains 103  
6 data points of which 68% represent paving stones in the Hemicycle and 32% are from  
7 the Via Biberatica. The lower ratio concentration contains 213 data points of which  
8 77% represent paving stones from the Hemicycle and 23% the Via Biberatica.  
9 Secondly, although there is no clear association between the data clusters in Figures  
10 12a and 12b, there is a tendency for the higher ratio concentration in Figure 12b to  
11 cluster around the Vallerano data in Fig 12a. Similarly there is a less well defined  
12 association between the lower ratio concentration in Figure 12b and the Villa Senni  
13 lavas in Figure 12a. From a proximity point of view a Vallerano source is possible as  
14 the quarries are close to the Tiber and are barely 12 km from central Rome as the crow  
15 flies (Fig.1). In support of this association Worthing et al. (2017) suggested that the  
16 Vallerano lavas were a possible source for paving stones in Ostia which is some 18km  
17 down stream of the Vallerano outcrops (Fig. 1). A Villa Senni source is slightly more  
18 problematic as the lava flows are further from central Rome (Fig.1). If proximity to  
19 construction sites was important then the Monte della Faete lavas are closer. Indeed one  
20 of them, the Capo di Bove flow, crosses into metropolitan Rome and the Via Appia is  
21 in places built on it (Fig.1).  
22  
23  
24

25 It was noted above that nine samples from Sabatini volcano plot in the Alban Hills field  
26 as defined in Figure 7 and 8 above. We have included these samples on Figure 12a  
27 where it can be seen that they tend to plot to the left of the lower ratio concentration,  
28 two in the Villa Senni field, three in the Monte della Faete field and three outside. This  
29 does not eliminate them completely as representing a possible source for the paving  
30 stones in this paper. However they are marginal to the main data points representing the  
31 Alban Hills. They also pose a problem of geographical location of these lava flows.  
32 Their latitude and longitude readings were abstracted from Conticelli et al. (1997) and  
33 their positions are plotted on Figure 1. They cluster around Lake Bracciano some 35 km  
34 north-west of Rome. We suggest that that this lack of proximity to Rome makes them a  
35 less likely source for the paving stones at Trajan's Market compared to the Alban Hills.  
36 We suggest that the latter association is more firmly established by the abundant data  
37 presented above.  
38  
39  
40

41 It was noted above that xenoliths were present in three paving stones in Area 3 of the  
42 Hemicycle. Tregila et al. (1995) stated that xenoliths are relatively common in the Villa  
43 Senni eruptive unit. One of the Area 3 xenolithic samples plots in the proposed Villa  
44 Senni group of Figure 12a and b and two in the proposed Vallerano group. However,  
45 these unclear associations lead us to conclude that unequivocal sourcing of the paving  
46 stones to individual eruptive phases on the Alban Hills is problematic. Unfortunately  
47 we did not have any Ta data so were unable to use the Th/Ta and Nb/Zr ratios to further  
48 refine our analysis. However with respect to the Vallerano lavas (Fig. 1), both the  
49 geochemistry and the proximity to the Tiber and to central Rome do lend weight to  
50 them as the possible source for lavas used in the Via Biberatica and the Hemicycle.  
51 Similarly the Vallerano lavas (Fig. 11a) do show the flattest curve in the spider  
52 diagrams of Figures 11 a-d. Further support comes from the suggestion of Worthing et  
53 al. (2017) that the Vallerano lavas were probably a source for paving stones at Ostia  
54 (Fig. 1). These two possible source - construction site associations imply that the  
55 paving stones were probably transported by barge (contrary to Delaine 2000: 135).  
56  
57  
58  
59  
60

## Summary and Conclusions

Sections of paving stones from the Via Biberatica and Trajan's Market Hemicycle were selected for geochemical analysis based on the geometric fit of the stones. The selected stones were then classified according to their petrographic features based on the presence or absence of phenocrysts, their modal composition and the presence of flow foliation. This analysis suggests significant petrographic differences between the paving stones from the Via Biberatica and Trajan's Market which can be explained by quarrying from different positions in the same lava flow or from different quarries or both. Clustering of the different petrographic types also allows some tentative conclusions to be drawn about the loading and unloading of stones from different parts of the source quarry or quarries. Geochemical analysis of the paving stones shows that they plot in well defined overlapping fields on XY plots. Comparisons with geological data for the Alban Hills, Sabatini and Vico on the same XY plots also show that both major and trace elements show a close association with the Alban Hills geological data. This association is confirmed by spider diagrams that normalise paving stone analyses to lava flow analyses for the four main effusive units of the Alban Hills: the Monte della Faete lavas, the Monte due Torri lavas, the Vallerano lavas and the Villa Senni lavas. However these spiders do not allow a definitive association to be established between the paving stones and any of the above effusive units. They simply confirm their overall connection with the Alban Hills. Further analysis using the ratios Zr/Y and Nb/Y (Marra et al 2011) suggests that the paving stones were quarried from at least two sources and that both these sources are represented in the Via Biberatica and the Hemicycle. A tentative association was also made between the Vallerano lavas and the Villa Senni lavas as possible sources. The former is considered to be a stronger candidate as the outcrops are close to the Tiber and to central Rome. In support of this, previous research suggested that a Vallerano source was used for paving stones at Ostia (Worthing et al 2017). If this is the case, it is probable that the paving stones were transported by barge to both Ostia and Rome. This conclusion posits a data-led alternative to the intuited assumption that the Capo di Bove lava flow was the source of paving and opens up questions of the use of the Tiber as a means of supplying paving stones to Rome contrary to assertions in the modern literature (DeLaine 2000: 135).

The utility of HHPXRF for this project and others of a similar type also needs some final discussion. It is clear from the above procedure that calibration of the Niton analyser is far from straightforward. Apart from the analytical capability of the machine there are two main problems that may influence the accuracy of the calibration. The first relates to the grain size of the standards and the paving stones. Normally groundmass analyses are measured when the Niton is used during calibration and field work. However the Niton window is about 2cm<sup>2</sup> which means that only a small area of the rock is irradiated. Thus the presence of phenocrysts or a coarser grain size may mean that some chemical components may not be included in the analysis which may therefore be unrepresentative of the bulk composition of the rock. The modal abundance of minerals hosting trace elements may also affect the measured concentrations of these elements. For example Zr is usually partitioned in the mineral Zircon (ZrSiO<sub>4</sub>) which may occur in very low modal abundance scattered throughout the rock matrix. Thus some zircons may be missed by a Niton analysis which will of course underestimate the concentration of Zr. A possible remedy is multiple analyses of the same rock but this is impossible when hundreds of paving stones need to be measured during fieldwork. Thus we conclude that finer grained aphyric rocks should

1  
2  
3 be selected but this is not always possible. The other issue, we encountered was  
4 instrument drift during fieldwork. We used COB1 to monitor Niton performance during  
5 fieldwork noting departures from expected values but we did not do this systematically.  
6 For example we could have referred to COB1 at fixed times of the day which may have  
7 revealed a temperature effect. However it is unclear what corrections could have been  
8 applied if this information had been available.  
9

10  
11 The calibration issues are also compounded by the analytical procedure used in lab-  
12 based XRF machines. This involves grinding the whole rock into a fine powder which  
13 is then melted with a flux to produce a fused glass disc for analysis. Thus the whole  
14 rock, including the phenocrysts is represented in the analysis and trace elements are  
15 also homogenized in the fused disc. These differences are relevant in the case for the  
16 Icelandic basalts used in the BIBROCEL calibration which were slightly porphyritic.  
17 Thus comparing Niton analyses with analyses obtained by lab-based XRFs can be  
18 problematic and may introduce errors in calibration. This may go some way to  
19 explaining some of the issues in making comparisons between lab-based data and that  
20 obtained with HHpXRF. Calibration protocols, taking averages of a number of  
21 readings, may partly compensate for these effects. However, we conclude that it is very  
22 difficult to obtain a perfect 1:1 calibration particularly with respect to trace elements.  
23 BIBROCEL is thus a best fit calibration.  
24  
25

26 To end on a more positive note; it is clear that when large amounts of Niton data  
27 obtained from volcanic rocks of known provenance are compared with literature based  
28 geological data of the same rocks, the agreement is good (e.g. Worthing et al. 2017),  
29 and there is an abundance of material available for further study and the production of  
30 data-led conclusions.  
31  
32

### 33 **Acknowledgement**

34  
35 We would like to thank Dr Christine Manning of the Earth Science Department at  
36 Royal Holloway and Bedford New College of the University of London who provided  
37 seven samples of Icelandic basalt with full XRF analyses. Without these samples we  
38 could not have calibrated the Niton. We also thank Professor Dave Wray of the  
39 University of Greenwich for providing a full XRF analysis of our field standard COB1  
40 and for useful discussions. The field work in Rome was greatly facilitated by two  
41 postgraduate students: Catherine Hoggarth and Tabitha Rose of the University of Kent.  
42 Research funds from the University of Kent are also gratefully acknowledged.  
43  
44  
45

### 46 **References**

- 47  
48 Alagna, K., Peccerillo, A., Martin, S. and Donati, C. 2010. Tertiary to Present  
49 Evolution of Orogenic Magmatism in Italy. In: (Eds.) Marco Beltrando, Angelo  
50 Peccerillo, Massimo Mattei, Sandro Conticelli, and Carlo Doglioni, The Geology of  
51 Italy: tectonics and life along plate margins, Journal of the Virtual Explorer, Electronic  
52 Edition, ISSN 1441-8142, volume 36, paper 18,  
53  
54  
55 Black, S., Browning, J., Laurence, R. 2004. From Quarry to Road: The supply of basalt  
56 for road paving in the Tiber Valley. In: Mecator Placidissimus The Tiber Valley in  
57 Antiquity Eds: Coarelli, F., Patterson, H. British School at Rome.  
58  
59  
60

1  
2  
3  
4 Boari, E., Avanzinelli, R., Melluso, L., Giordano, G., Mattei, M., Arnaldo, A., De  
5 Benedetti, A.A., Morra, V., Conticelli, S. 2009. Isotope geochemistry (Sr-Nd-Pb) of  
6 leucite-bearing volcanic rocks from “Colli Albani” volcano, Roman Magmatic  
7 Province, Central Italy: inferences on volcano evolution and magma genesis. *Bulletin*  
8 *of Volcanology* 71, 977-1005.  
9

10  
11 Capedri, S., Grandi, R. 2003. Trachytes Used for Paving Roman Roads in the Po Plain:  
12 Characterization by Petrographic and Chemical Parameters and Provenance of Paving  
13 stones. *Journal of Archaeological Science* 30, 491-509.  
14

15  
16 Conticelli, S., Francalanci, L., Manetti, P., Cioni, R., Sbrana, A. 1997. Petrology and  
17 geochemistry of the ultrapotassic rocks of the Sabatini Volcanic District, central Italy:  
18 the role of evolutionary processes in the genesis of variably enriched alkaline magmas.  
19 *Journal of Volcanology and Geothermal Research* 75, 107-136.  
20

21  
22 Conticelli, S., Carlson RW., Widom E., Serri G. 2007. Chemical and isotopic  
23 composition (Os, Pb, Nd and Sr) of Neogene to Quaternary calc-alkalic, shoshonitic  
24 and ultrapotassic mafic rocks from the Italian peninsula: Inferences on the nature of  
25 their mantle sources. *Geological Society of America, Special Paper*, 418, 171-202.  
26

27  
28 Conticelli, S., Laurenzi, M.A., Mattei, M., Avanzinelli, R., Melluso L., Tommasini, S.,  
29 Boari E., Cifelli, F. Perini, G., 2010a. Leucite bearing (kamagfugitic/leucitic) and free  
30 lamproitic ultrapotassic rocks and associated shoshonites from Italy: constraints on  
31 petrogenesis and geodynamics. In: (Eds.) Marco Beltrando, Angelo Peccerillo,  
32 Massimo Mattei, Sandro Conticelli, and Carlo Doglioni, *The Geology of Italy:*  
33 *tectonics and life along plate margins*, *Journal of the Virtual Explorer, Electronic*  
34 *Journal of Virtual Explorer*, 36, Paper 20, 1-95.  
35

36  
37 Conticelli, S., Boari E, Avanzinelli, De Benedetti, A.A., Giordano, G., Mattei, M,  
38 Mellusco L, Morra V. 2010b. Geochemistry, isotopes and mineral chemistry of the  
39 Colli Albani volcanic rocks: constraints on magma genesis and evolution. From:  
40 Funicello, R. and Giordano, G. (eds) *The Colli Albani Volcano. Special Publications*  
41 *of IAVCEI*, 3, 107-139. Geological Society of London, London.  
42

43  
44 DeLaine, J. 1997. The Baths of Caracalla. A study in the design, construction of large-  
45 scale building projects in imperial Rome (*Journal of Roman Archaeology* Suppl.25,  
46 Portsmouth RI.  
47

48  
49 DeLaine, J. 2000. Building the Eternal City: the construction industry of imperial  
50 Rome, in J. Coulston and H. Dodge (eds) *Ancient Rome: The Archaeology of the*  
51 *Eternal City*, 119-141, Oxbow: Oxford.  
52

53  
54 Frahm, E. and Doonan, R.C.P. 2013. The technological versus methodological  
55 revolution of portable XRF in archaeology. *Journal of Archaeological Science* 40,  
56 1425-1438.  
57

58  
59 Gaeta, M., Freda, C, Christiansen, J.N., Dallai, L., Marra, F., Karner, D.B., Scarlato, P.  
60 2006. Time-dependant geochemistry of clinopyroxene from the Alban Hills (Central  
Italy): Clues to the source and evolution of ultrapotassic magmas. *Lithos* 86, 330-346.

1  
2  
3  
4 Gaeta, M., Freda, C., Marra, F., Di Rocco, T., Gozzi, F., Arienzo, I., Giaccio, B.,  
5 Scarlato, P. 2011. Petrology of the most recent ultrapotassic magmas from the Roman  
6 Province (Central Italy) *Lithos*, 127, 298-308.

7  
8 Gaeta, M., Freda, C., F., Marra, F., Arienzo, I., Gozzi, F., Jicha, B., Di Rocco, T. 2016.  
9 Palaeozoic metasomatism at the origin of Mediterranean ultrapotassic magmas:  
10 Constraints from time dependant geochemistry of Colli Albani volcanic products  
11 (Central Italy) 2016. *Lithos* 244, 151-164.

12  
13  
14 Giordano, G., De Benedetti, A.A., Diana, A., Diano, G., Gaudio, F., Marasco, F.,  
15 Miceli, M., Mollo, S., Cas, R.A.F., Funicello, R. 2006. The Colli Albani mafic caldera  
16 (Roma Italy): Stratigraphy, structure and petrology. *Journal of Volcanology and*  
17 *Geothermal Research* 155, 49-80.

18  
19  
20 Gozzi, F. 2012. Ultrapotassic lava flows from Colli Albani Volcanic District shed light on  
21 the origin of calcite bearing magmas. PhD thesis, Sapienza University of Rome.

22  
23 Gozzi, F., Gaeta, M., Freda, C., Mollo, S., Di Rocco, T., Marra, F., Dallai, L., Pack, A.  
24 2014. Primary Magmatic calcite reveals origin from crustal carbonate. *Lithos* 190-191,  
25 191-203.

26  
27  
28 Karner, D.B., Marra, F., Renne, P., 2001. The History of Monti Sabatini and Alban  
29 Hills Volcanoes: Groundwork for assessing Volcanic-Tectonic Hazards for Rome.  
30 *Journal of Volcanology and Geothermal Research* 107, 185-219.

31  
32 Laurence, R. 1999. *The Roads of Roman Italy, Mobility and Cultural Change*.  
33 Routledge, pp 221.

34  
35 Laurence, R. 2004. The Economic Exploitation of Geological Resources in the Tiber  
36 Valley: Road Building. In: *Bridging the Tiber, Approaches to Regional Archaeology in*  
37 *the Middle Tiber Valley* Ed: Patterson, H. *Archaeological Monographs of the British*  
38 *School at Rome*.

39  
40  
41 Marra, F., Karner, D.B., Freda, C., Gaeta, M., Renne, P. 2009. Large mafic eruptions at  
42 Alban Hills Volcanic District (Central Italy): Chronostratigraphy, petrography and  
43 eruptive behaviour. *Journal of Volcanology and Geothermal Research* 179, 217-232.

44  
45 Marra, F., Deocampo, D., Jackson, M.D., Ventura, G. 2011. The Alban Hills and Monti  
46 Sabatini volcanic products used in ancient Roman masonry (Italy) An integrated  
47 stratigraphic, archaeological, environmental and geochemical approach. *Earth Science*  
48 *Reviews*, 108, 115-136.

49  
50  
51 Marra, F., Sottili, G., Gaeta, M., Giaccio, B., Jicha, B., Massotta, M., Palladino, D.M.,  
52 Deocampo, D., 2014. Major explosive activity in the Sabatini Volcanic District (central  
53 Italy) over the 800-390 ka interval: geochronological-geochemical overview and  
54 tephrostratigraphic implications. *Quaternary Science Reviews*, 94, 74-101.

55  
56  
57 Peccerillo, A. 2005. The Roman Province. In: *Plio-Quaternary Volcanoes in Italy*.  
58 *Petrology, Geochemistry, Geodynamics*. Springer, pp 70-106.

1  
2  
3  
4 Perini, G., Conticelli, S., Francalanci, L., Davidson, J.P. 2000. The relationship  
5 between potassic and calc-alkaline post-orogenic magmatism at Vico volcano, central  
6 Italy. *Journal of Volcanology and Geothermal Research* 95, 247-272.  
7

8 Perini, G., Francalanci, L., Davidson, J.P., Conticelli, S. 2004. Evolution and Genesis  
9 of Magmas from Vico Volcano, Central Italy: Multiple Differentiation pathways and  
10 Variable Parental Magmas. *Journal of Petrology*, 45, 139-182.  
11

12  
13 Sottili, G., Palladino, D.M., Marra, F., Jicha, B., Karner, D.B., Renne, P., 2010.  
14 Geochronology of the most recent activity in the Sabatini Volcanic District, Roman  
15 Province, Central Italy. *Journal of Volcanology and Geothermal Research* 196, 20-30.  
16

17  
18 Trigila, R., Agosta, E., Currado, C., De Benedetti, A.A., Freda, C., Gaeta, M.,  
19 Palladino, D.M., Rosa, C. 1995. Petrology. In: *The Volcano of the Alban Hills*.  
20 *Tipografia SGS, Roma*, 95-165.  
21

22 Worthing, M., Browning, J., Laurence, R., Bosworth, L. 2017. Geochemical Methods for  
23 Sourcing Lava Paving Stones from the Roman roads of Central Italy. *Archaeometry*. In  
24 Press.  
25  
26  
27  
28  
29  
30  
31  
32  
33  
34  
35  
36  
37  
38  
39  
40  
41  
42  
43  
44  
45  
46  
47  
48  
49  
50  
51  
52  
53  
54  
55  
56  
57  
58  
59  
60



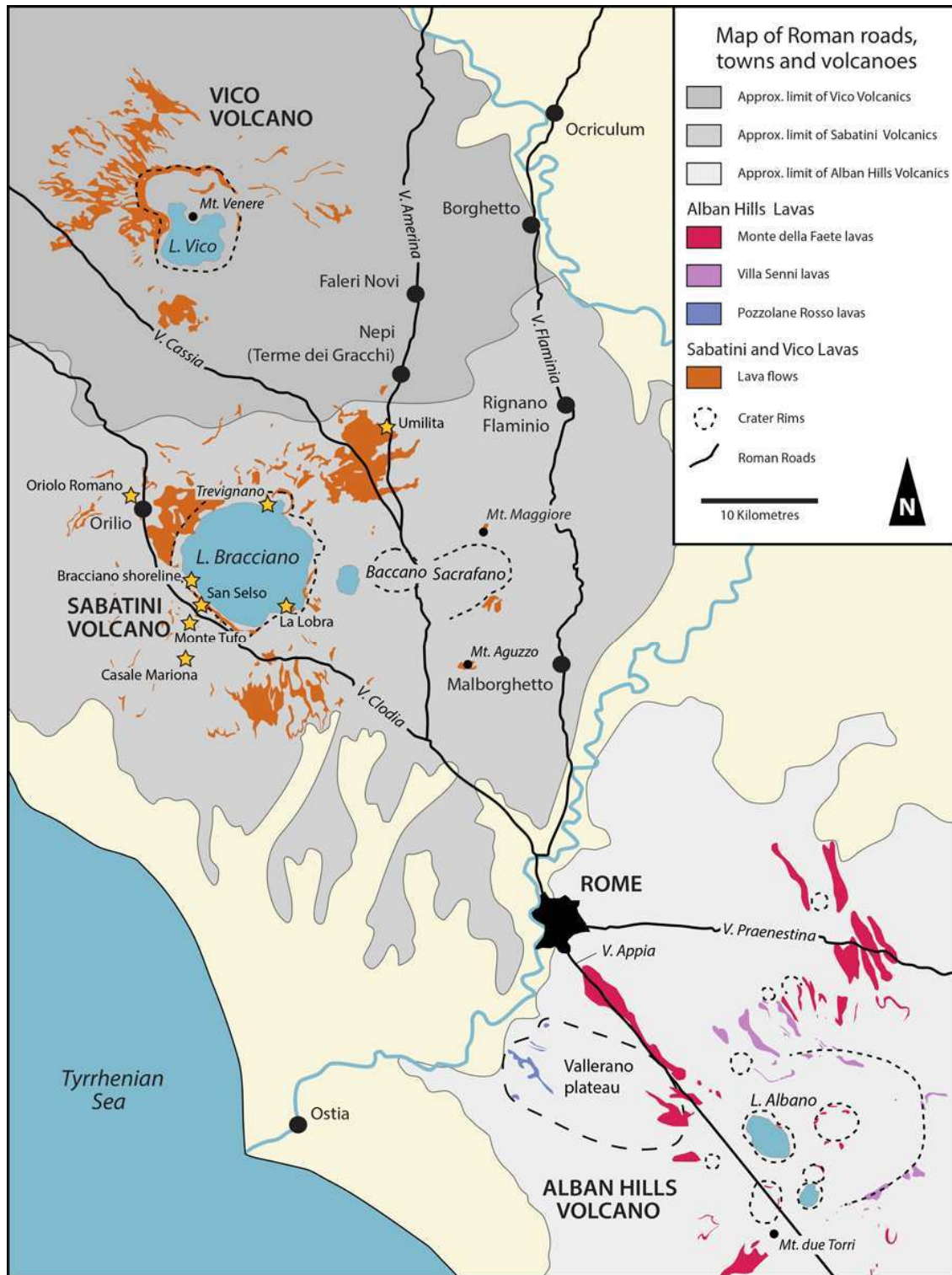


Fig.1.

1  
2  
3  
4  
5  
6  
7  
8  
9  
10  
11  
12  
13  
14  
15  
16  
17  
18  
19  
20  
21  
22  
23  
24  
25  
26  
27  
28  
29  
30  
31  
32  
33  
34  
35  
36  
37  
38  
39  
40  
41  
42  
43  
44  
45  
46  
47  
48  
49  
50  
51  
52  
53  
54  
55  
56  
57  
58  
59  
60

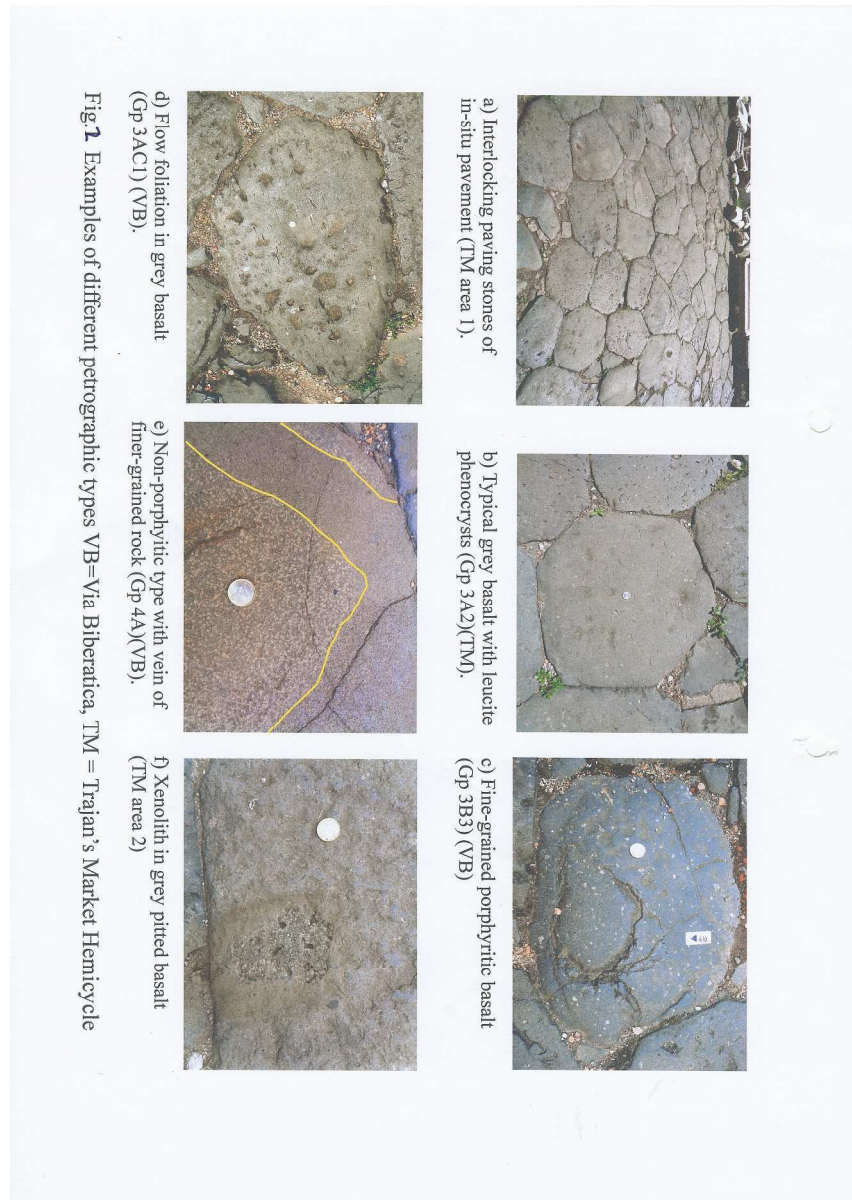


Fig. 4. Photographs of different petrographic types VB = Via Biberatica, TM = Trajan's Market Hemicycle. Key to symbols in Table 1.

208x293mm (300 x 300 DPI)

1  
2  
3  
4  
5  
6  
7  
8  
9  
10  
11  
12  
13  
14  
15  
16  
17  
18  
19  
20  
21  
22  
23  
24  
25  
26  
27  
28  
29  
30  
31  
32  
33  
34  
35  
36  
37  
38  
39  
40  
41  
42  
43  
44  
45  
46  
47  
48  
49  
50  
51  
52  
53  
54  
55  
56  
57  
58  
59  
60

1  
2  
3  
4  
5  
6  
7  
8  
9  
10  
11  
12  
13  
14  
15  
16  
17  
18  
19  
20  
21  
22  
23  
24  
25  
26  
27  
28  
29  
30  
31  
32  
33  
34  
35  
36  
37  
38  
39  
40  
41  
42  
43  
44  
45  
46  
47  
48  
49  
50  
51  
52  
53  
54  
55  
56  
57  
58  
59  
60

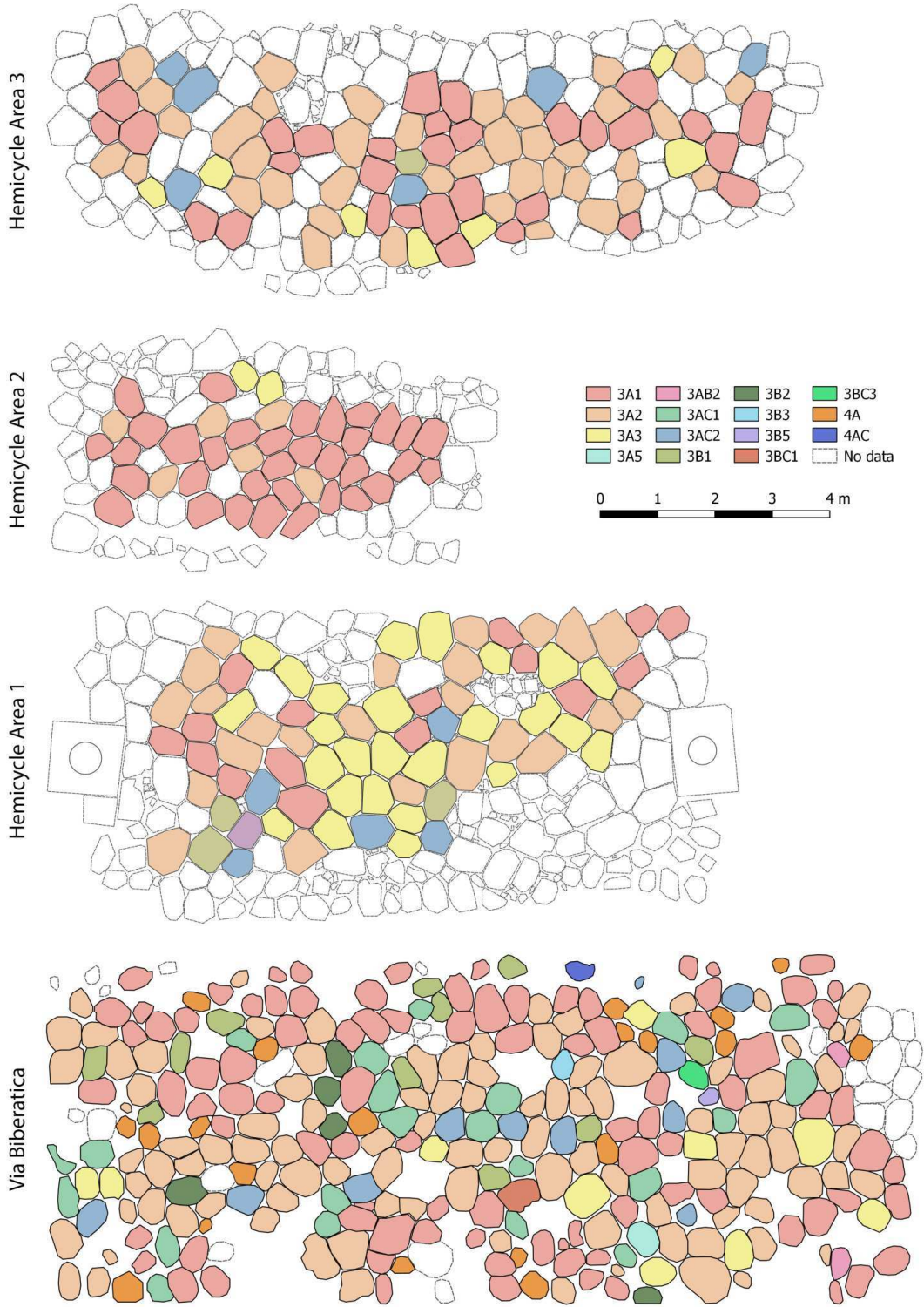


Fig.4. Areal distribution of the different petrographic types in the three areas of the Hemicycle and the Via Biberatica.

Group	Symbol	Definition
<b>3Ax</b>	3	Porphyritic
	A	Groundmass visible with naked eye
	x = 1-5	Percentage of phenocrysts
<b>3ACx</b>	3	Porphyritic
	A	Groundmass visible with naked eye
	C	Flow foliation present
	x = 1-3	Percentage of phenocrysts
<b>3Bx</b>	3	Porphyritic
	B	Groundmass not visible with naked eye
	x = 1-5	Percentage of phenocrysts
<b>3BCx</b>	3	Porphyritic
	B	Groundmass not visible with naked eye
	C	Flow foliation present
	x = 1-3	Percentage of phenocrysts
<b>4A</b>	4	Phenocrysts absent
	A	Groundmass visible with naked eye

**Table 1.** Examples of criteria for paving stone petrographic classification.

	Alban Hills*		VB	TM
<b>SiO<sub>2</sub></b>	54.80	54.90	50.41	49.86
<b>TiO<sub>2</sub></b>	0.05	0.05	0.35	0.30
<b>Al<sub>2</sub>O<sub>3</sub></b>	22.90	23.30	15.40	15.53
<b>Fe<sub>2</sub>O<sub>3</sub></b>	0.71	0.67	1.11	0.69
<b>MgO</b>	bdl	bdl	0.01	0.00
<b>CaO</b>	bdl	bdl	1.49	0.98
<b>Na<sub>2</sub>O</b>	0.1	0.08	nd	nd
<b>K<sub>2</sub>O</b>	21.00	21.30	16.30	16.56
<b>P<sub>2</sub>O<sub>5</sub></b>	nd	nd	0.28	0.45
<b>Sr ppm</b>	2114	423	286	116
<b>Ba ppm</b>	182	2180	626	544

Table 2. Leucite analyses (\*after Boari et al. 2009), bdl = below detection limits, nd = not determined. VB = Via Biberatica, TM =Trajan's Market Hemicycle. VB and TM are averages of 5 analyses.

**Table 2.** Niton leucite analyses (VB and TM) compared with microprobe analyses of leucites from the Alban Hills after Boari (2009).

Peer Review